Sandeep K M, 2025, 13:6
ISSN (Online): 2348-4098
ISSN (Print): 2395-4752

International Journal of Science, Engineering and Technology
An Open Access Journal

Frequency-Dependent AC Conductivity and Dielectric Studies of PPy/WO_3 Nanocomposites for Frequency-Tunable Dielectric Devices

Sandeep K M, J S Ashwajeet, Raghavendra M N.
Department of Studies in Physics, Davangere University, Shivagangothri, Davanagere – 577007, Karnataka.

Abstract- In this study, polypyrrole/tungsten trioxide (PPy/WO_3) nanocomposites were synthesized by chemical oxidative polymerization and systematically analyzed for their frequency-dependent AC conductivity and dielectric properties. X-ray diffraction confirmed the successful integration of nanocrystalline WO_3 within the amorphous PPy matrix, with crystallite sizes between 61.9 and 74.5 nm. Dielectric measurements showed that increasing WO_3 content significantly enhanced both permittivity (ε′) and dielectric loss (ε″), particularly at low frequencies—an effect attributed to Maxwell–Wagner–Sillars interfacial polarization. AC conductivity increased monotonically with frequency, followed Jonscher's universal power law ($0.22 \leq s \leq 0.50$), and rose from ~$10^{-}3$ to $10^{-}1$ S·cm^{-1} with frequency and optimal WO_3 loading, consistent with hopping and tunneling of localized charge carriers through percolative pathways. Electric modulus and Nyquist impedance analyses revealed pronounced non-Debye relaxation, a broad distribution of relaxation times, and strong composition dependence of bulk and interfacial resistances. Notably, an intermediate WO_3 content offered the best balance between enhanced interfacial polarization and the formation of continuous conducting networks. These results demonstrate that precise control of WO_3 loading enables effective tuning of polarization mechanisms, relaxation dynamics, and AC conduction in PPy, positioning PPy/WO_3 nanocomposites as promising candidates for frequency-tunable dielectric components, capacitive sensors, and compact energy storage devices.

Keywords: polypyrrole; tungsten oxide; electric studies; Jonscher power law.

I. INTRODUCTION

Polypyrrole (PPy) is an important intrinsically conducting polymer with tunable conductivity, good environmental stability, and promising use in sensors, antistatic coatings, and energy-storage devices, yet its dielectric and high-frequency transport properties in pristine form remain inadequate for many advanced applications [1–3]. The development of next-generation functional materials therefore increasingly relies on hybrid structures that synergistically combine the advantages of organic and inorganic phases. In this context, incorporating inorganic oxide nanofillers into PPy has emerged as an effective strategy to enhance permittivity, thermal and environmental stability, and charge-transport pathways via strong interfacial polarization [4,5].

Tungsten trioxide (WO_3) is an n-type transition-metal oxide with a moderate band gap and a relatively high dielectric constant. Tungsten trioxide (WO_3) is a multifunctional transition metal oxide recognized for its impressive electronic, optical, and catalytic properties, making it highly valuable in various technological fields. Its significant electrochromic behavior is exploited in smart windows, anti-glare mirrors, and adaptive optical devices due to its excellent optical modulation and chemical stability [6].

Recent advances show that nanostructuring and composite formation greatly enhance WO_3's electrochromic and photocatalytic performance, and WO_3-based materials are highly efficient for photocatalytic degradation of water pollutants [7]. and show promise as electrode materials in energy storage devices due to their favorable redox properties and stability [8]. It also has rich electrochromic and gas-sensing properties and behaves like a semiconductor. This makes it a very good choice as an electron-accepting filler for PPy matrices [9–11]. Polymer/oxide interfaces with WO_3 are likely to change the microstructure, make the

conducting paths denser, and encourage Maxwell–Wagner–Sillars interfacial polarization and hopping-type conduction.

This will make both DC and AC electrical responses better [12–15]. Prior investigations into WO_3-based polymer nanocomposites, including PEG/CS–WO_3, PVA/MWCNT/WO_3, and PMMA/PANI–WO_3, as well as bulk WO_3, have demonstrated pronounced frequency dispersion, correlated-barrier-hopping behavior, and substantial enhancement of dielectric and conductive properties, highlighting the potential of WO_3 as an active dielectric or conductive filler [6,12,16,17]. Despite these advancements, the majority of reported WO_3 composites utilize insulating or weakly conducting hosts, or alternative conducting matrices such as PVA, PANI, PIn, and PMMA/PANI blends [18].

Motivated by these considerations, the present study focuses on PPy/WO_3 nanocomposites synthesized via chemical oxidative polymerization in the presence of an oxidizing agent; pure PPy and its WO_3-loaded counterparts are characterized by X-ray diffraction (XRD) and room-temperature, frequency-dependent AC measurements to establish their structural and electrical features. Detailed dielectric and impedance analyses, including Nyquist plots, Z′/Z″ evaluation, and electric-modulus formalism, are employed to probe frequency-dependent conductivity, charge-transfer resistance and relaxation dynamics. These investigations provide an integrated understanding of how WO_3 incorporation modulates the dielectric response of PPy, correlating structural characteristics with electrical performance and underscoring the potential of PPy/WO_3 nanocomposites for frequency-tunable dielectric components, capacitive sensors, and compact energy storage devices.

II. EXPERIMENTAL STUDIES

Materials:

The Pyrrole AG grade purity 99.9%, Ammonium persulphate AR grade [NH4H2SO8], purity 99.9%, Hydrochloric acid [HCL], purity 99.9%, Acetone [C3H6O], purity 99.9% from Nice Chemical Private Limited and Tungsten (IV) oxide (WO_3) AR grade from Loba Chemie Pvt. Limited, purity of 99% and double deionized water were also used for the preparation of required compounds.

Synthesis of Polypyrrole (PPy):

A chemical oxidative polymerization procedure was used to synthesize PPY. 0.5 M of pyrrole was dissolved in 100 ml of 0.5M solution of HCl. Pre-cooled 1M ammonium persulphate (APS) was added dropwise to the pyrrole-acid mixture for about 3 hours. Polymerization was carried out at a temperature of 0°C to 5°C with controlled stirring for 5 h. A dark black-colored precipitate. Thus formed. The obtained black polypyrrole was washed with 1N HCl to remove unreacted pyrrole. Then deionized water to remove APS in the matrix, then acetone to recover any organic impurities. The filtered material was dried at 600°C for 24 h and stored in an airtight container.

Fig. 1. Chemical oxidative polymerization of PPy with WO_2 nanocomposite.

Synthesis of PPY–WO_3

PPY–WO3 was synthesized via a chemical oxidation method using pyrrole, ammonium persulphate, hydrochloric acid, and WO3. A 0.5 M aqueous pyrrole solution was mixed with 0.5 M hydrochloric acid to form a PPY solution. To keep the WO_3 suspended in the solution, the PPY solution was mixed with WO_3 at vigorous stirring. With this 1 M of

solution, ammonium persulphate was added dropwise with continuous stirring for 4–5 h at 0–50C respectively. The black-colored precipitate was obtained, filtered, and washed several times with deionized water. Finally, the residue was dried in an oven for 24 hours. PPY/WO_3 composites were synthesized in different percentage weights in which the concentration of tungsten oxide (5%, 10%, & 15%) , Wt% was varied.

III. RESULTS AND DISCUSSIONS

X-Ray Diffraction Studies:

With a Rigaku Corporation [Model-Smart Lab 3Kw Ser. No. BD63000074] X-ray diffractometer system, which uses Cu (kα) radiation with a wavelength of 1.5406 Å, with a scanning speed of 5 deg/min.

The XRD patterns of PYW-0 to PYW-3 clearly show that PPy/WO_3 nanocomposites have formed. PYW-0 (pure PPy) has only a broad amorphous halo centered at about 24–26° (Cu Kα), which is typical of polymer chains that are not well ordered. [19]. When WO_3 (PYW-1 to PYW-3) is added, a series of sharp reflections appear and get stronger over time. These reflections can be matched to monoclinic γ-WO_3 in JCPDS card numbers 33-1387 and 71-0131 [2,20].

The characteristic diffraction peaks are observed at approximately 23.6° (020), 26.6° (120), 28.71° (022), 34.1° (220), 35.6° (220), 41.7° (222), 50.0° (400), 55.5° (402), 59.0°, 62.1° (421), and 76.81° (424), in addition to less intense high-angle reflections [21]. The progressive growth of these WO_3 peaks alongside the diminishing dominance of the polymer halo indicates increasing crystalline oxide content and improved phase development within the PPy matrix, any slight 2θ shifts or peak broadening can be ascribed to nanocrystalline size, macrostrain, and interfacial stresses at the polymer–oxide boundary.

Using the Debye-Scherrer formula, interplanar spacing, d, lattice constant, a, and average crystallite size, D, were determined and tabulated in table 1.
The lattice parameter's such as lattice constant, a, varying from 6.66 to 7.49 Å, interplanar distance, d is shown 2.18 Å to 2.35 Å and the average crystallite size, D is found 61.9 nm to 74.5 nm and confirm the WO3 nanocomposites.

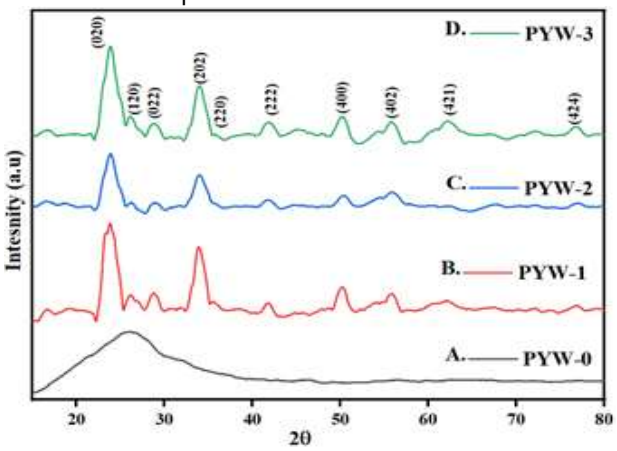

Fig. 2. XRD patterns of PPy/WO_3 (0-15%) nanocomposite.

Table 1. Interplanar distance d, lattice constant, a, & average crystallite size for PPy/WO_3 nanocomposite.

SAMPLE CODE	d in Å	a in Å	D in nm.
PYW-1	2.35	8.19	61.9
PYW-2	2.25	8.51	74.5
PYW-3	2.18	7.86	65.2

Electrical Studies:

Dielectric constant (ε'):

The dielectric constant (ε') of PPy/WO_3 nanocomposites (PYW-0, to PYW-3, WO_3 concentration x = 5% to 25%) as a function of frequency (ln F). For all compositions, ε′ decreases as the frequency goes up (Fig. 3). [5,22]. This is a common behavior of dielectric materials because dipoles and charge carriers can't keep up with the quickly changing electric field at higher frequencies.

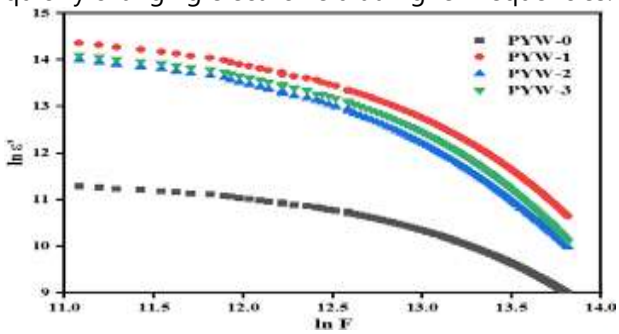

Fig. 3. Variation of dielectric constant, ε′ as a function of frequency, lnF for PPy/WO_3 nanocomposite (X = 0.5, 10, & 15 wt %)

The dielectric constant of pristine PPy (PYW-0) is the lowest across the entire frequency range. Adding WO_3 (PYW-1, PYW-2, PYW-3) makes ε′ much higher at all frequencies. This enhancement is primarily due to Maxwell–Wagner–Sillars interfacial polarization, charge accumulation at the polymer/filler interfaces, and the active contribution of WO_3 particles in strengthening the overall polarization response. Nanocomposites with moderate WO_3 loading (~10–15 wt%) show the highest ε′ values. This means that there is an ideal amount of filler beyond which too much WO_3 can break the conducting network or add more scattering centers. In general, these results show that doping PPy with WO_3 changes and improves its dielectric properties. The frequency-dependent relaxation behavior we saw is in line with the Maxwell–Wagner model and Koop's phenomenological theory [15,23].

Dielectric Loss Studies:

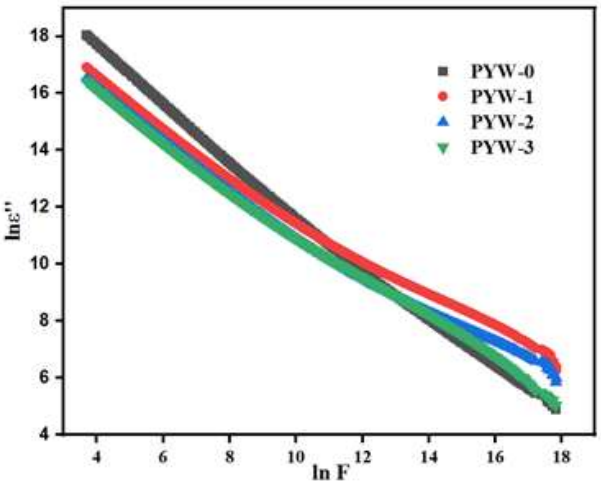

Fig. 4. Variation of dielectric loss, ε″ as a function of frequency, lnF, for PPy/WO_3 nanocomposite (X = 0.5, 10, & 15 wt %).

A Similar trends are seen for ε″ (Fig. 4), where the dielectric loss ε″ in PPy/WO_3 nanocomposites (PYW-0, to PYW-3) decreases monotonically with ln F, closely resembling the ε′–frequency behavior [24], Maxwell-Wagner-Sillars interfacial polarization and space-charge accumulation at PPy/WO_3 interfaces increase ε′ and ε″ at low frequencies, resulting in significant energy loss [25]. As frequency rises, polarization mechanisms and charge carriers struggle to adapt to the fast-alternating electric field, resulting in reduced carrier migration and a sharp drop in ε″ before plateauing [16-18]. The ε″ values of composites with moderate WO_3 loading (PPy-W1 to W3, ≈5–15 wt%) are consistently higher than those of pristine PPy, indicating a well-dispersed, interface-rich network that encourages dielectric loss and interfacial polarization [24,26]. Overall, dielectric relaxation processes in conducting polymer-based nanocomposites are characterized by a uniform decrease in ε″ with increasing frequency.

AC Conductivity Studies:

AC conductivity (σ) varies with frequency (ln ω) for PPy/WO_3 nanocomposites (PYW-0 to PYW-3, with WO_3 concentrations of (5-15%) are shown in Fig 5. The conductivity pattern reveals two distinct regions: σ is essentially constant at lower frequencies and sharply increases at higher frequencies. Jonscher's universal power law well explains this trend:

$$\sigma(\omega)=\sigma dc+A\omega s, \quad (1)$$

where the frequency exponent is denoted by s (0 < s < 1), A is a pre-exponential factor, and σdc is the frequency-independent conductivity [27].

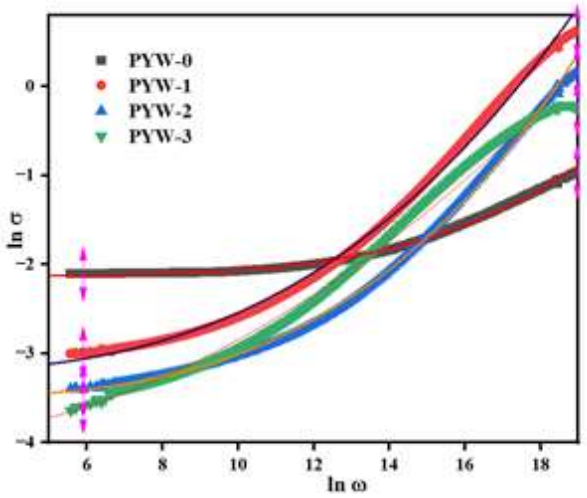

Fig. 5. Variation of ac conductivity, σ, as a function of frequency, ln▪ for PPy/WO_3 nanocomposite (X = 0.5, 10, & 15 wt %).

The variation of AC conductivity (ln σ) with frequency (ln F) for pristine polypyrrole (PYW-0) and its WO_3-doped nanocomposites (PYW-1, PYW-2, and PYW-3). For all compositions, AC conductivity increases

monotonically with frequency (Fig.5), which is characteristic of disordered conducting polymers and is associated with the enhanced hopping probability of charge carriers between localized states at higher frequencies.

The nearly flat region at low frequencies corresponds to the DC conductivity (σdc), dominated by long-range translational motion of polarons and bipolarons along the PPy backbone. At higher frequencies, σac rises due to charge carriers tunnelling and hopping between polaronic sites located on the PPy–WO_3 interfaces and within the polymer matrix [28]. Across the entire frequency range, pristine PPy (PYW-0) exhibits the lowest conductivity, while the WO_3-doped samples show significantly higher values, with the conductivity enhancement correlating positively with WO_3 content.

The AC conductivity of the nanocomposites lies in the range of approximately $10^{-}3–10^{-}1$ S/cm , and the comparatively higher conductivity values of PYW-1, PYW-2, and PYW-3 indicate that moderate WO_3 loading improves charge transfer through better interfacial contact and reduced carrier scattering. However, excessive filler content may promote agglomeration, reducing the effectiveness of conductive pathways and hindering carrier transport. This frequency-dependent behavior is consistent with a hopping conduction mechanism, as described by small-polaron tunnelling and correlated barrier hopping models commonly applied to conducting polymer composites [29], and highlights the crucial role of filler concentration and interfacial polarization in governing both dielectric relaxation and conduction processes.

In the region between ln(ω) = 13 to ln(ω) = 18, the graph shows a pronounced increase in ln(σ) for all four samples, indicating a strong frequency-dependent enhancement in AC conductivity. This region likely corresponds to the high-frequency regime, where localized charge carriers gain sufficient energy to overcome potential barriers and participate in hopping conduction or interfacial polarization. The study reveals that localized charge carriers dominate the conduction mechanism, evidenced by the increase in AC conductivity as frequency decreases, along with simultaneous drops in dielectric loss and dielectric constant. The filler (WO_3) concentration is a critical factor, with the polymer nanocomposite achieving its optimal dielectric and conduction performance at mid-level loading. Higher filler concentrations, however, cause nanoparticle agglomeration, increasing interchain distances and hindering the hopping of charge carriers, ultimately resulting in lower conductivity [30][31].

Table 2. Variation of ac conductivity for 1000 kHz, 1 MHz, 10 MHz, 30 MHz, 40 MHz & frequency exponent (s) for PPy/WO_3 nanocomposite (X = 0.5, 10, & 15 wt%).

Sample CODE	Frequency exponent (s)	DC	Conductivity ‧ in Ω^{-1} cm^{-1}				
			KHz 10^{-2}	1 MHz × 10^{-2}	10 MHz × 10^{-2}	30 MHz × 10^{-2}	40 MHz × 10^{-2}
PYW-0	0.22	0.120	12.1	18.4	31.71	41.4	45.16
PYW-1	0.40	0.045	6.2	47.8	135.42	191.3	197.9
PYW-2	0.33	0.032	4.2	25.1	77.90	124.8	131.9
PYW-3	0.50	0.024	4.1	30.8	64.31	80.3	81.10

Dielectric Studies

Electrical Modulus:

The real (M′) and imaginary (M″) (inset) parts of the electric modulus for PPy/WO_3 nanocomposites show how the amount of WO_3 affects relaxation dynamics (Fig. 7). For all compositions (PYW-0 to PYW-3, 0–15 wt% WO_3), M′ and M″ remain close to zero and are nearly frequency-independent in the low-frequency region. This means that the effective permittivity is very large and is mostly caused by electrode and space-charge polarization. This is where mobile charge carriers can follow the slowly changing field and build up at interfaces and grain boundaries [32]. As the frequency goes up (ln F ≈ 13–14), electrode

polarization gets weaker, the bulk response takes over, and both M′ and M″ go up sharply.

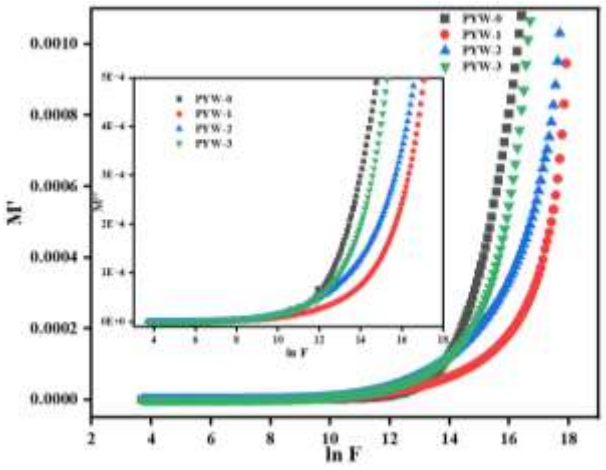

Fig. 7 Variation of M' and M' as a function of frequency for PYW-0 to PYW-3 nanocomposites (x = 5%, 10%, 15%, 20% and 25%).

This is a change from long-range translational motion to localized hopping of carriers, which lowers effective permittivity and raises modulus. Pristine PPy (PYW-0) has the highest M′ and M″ values. On the other hand, WO_3-doped samples have a lower modulus, especially when the WO_3 content is low (≈5 wt%). This is because the interfacial polarization is stronger, the dielectric permittivity is higher, and more hopping pathways are formed along the PPy/WO_3 interfaces. For intermediate loadings (PYW-2 and PYW-3, 10–15 wt%), the M′ and M″ curves shift to higher values in the mid–high-frequency region and start earlier than for lightly or heavily filled samples.

This suggests that moderate WO_3 content creates an optimal interfacial network that encourages Maxwell–Wagner–Sillars interfacial polarization and segmental-chain relaxation along well-connected polymer/oxide pathways. At even higher WO_3 levels, a small rise in modulus and a tendency for stiffness can be linked to filler agglomeration and limited chain mobility, which lower the effective interfacial area [33,34]. The smooth, non-Lorentzian evolution of M′ and the lack of a sharp M″ peak in the measured frequency window suggest that the relaxation times are spread out and that the system doesn't follow the Debye model. This is a sign of structurally heterogeneous polymer/oxide systems where grain and grain-boundary contributions are the most important [35–38].

The complex electric-modulus plot for PPy/WO_3 nanocomposites (PYW-0 to PYW-3, 0–15 weight percent WO_3) is displayed in Fig. 8, as M″ plotted versus M′ throughout the measured frequency range. The loci for all compositions start near the origin and increase toward higher M′ and M″ with frequency, indicating that bulk dielectric relaxation, not direct current conduction, drives the response. The curves show distortion and stretching, indicating non-Debye relaxation and a wide relaxation time distribution in the PPy–WO_3 network due to structural heterogeneity and grain-boundary effects. The sample PYW-1 (5 wt% WO_3) has the shortest locus, lowest M′ and M″ values, and improved charge transport due to well-dispersed WO_3 and efficient polymer/filler pathways.

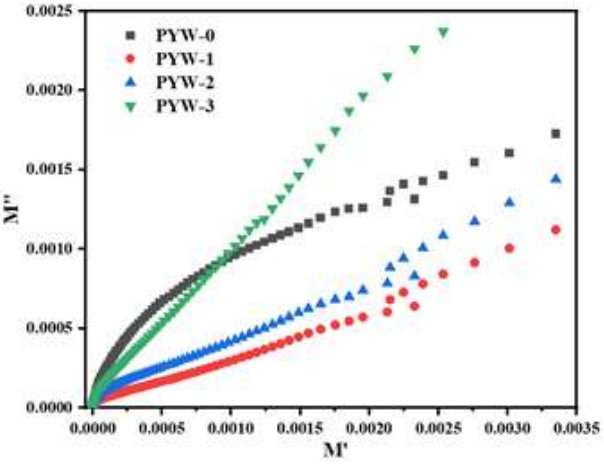

Fig. 8. The complex modulus (M′ vs. M″) for PYW-0 to PYW-3 nanocomposites (x = 5%, 10% & 15%,).

In contrast, higher WO_3 loadings (10 and 15 wt%) lead to extended arcs and increased M″, indicating enhanced energy dissipation and interfacial/space-charge polarization due to filler agglomeration and limited chain mobility. The incorporation of WO_3 significantly alters the relaxation dynamics of PPy, as shown by the M′–M″ behavior. Moderate doping at 5 wt% improves dielectric performance, while excessive loading causes loss and non-Debye interfacial polarization.

Impedance analysis:

The complex impedance of PPy/WO_3 nanocomposites as a function of ln F is shown in Fig.9., (PYW-0 to PYW-3, 0–15 wt% WO_3). Z′ consistently decreases with increasing ln F, signifying a transition from primarily resistive behavior at low frequencies to more capacitive or conductive behavior at higher frequencies [36,39]. At low frequencies, the impedance remains high and nearly constant, attributed to limited charge mobility, significant interfacial/electrode polarization, and space-charge accumulation. In this context, undoped PPy (PYW-0) demonstrates a substantial Z′, whereas the 5 wt% WO_3 sample (PYW-1) exhibits the highest Z′ among the doped compositions, indicating increased resistance to charge flow[40,41]. With increasing frequency, the Z′ for WO_3-loaded samples exhibits a more pronounced decrease compared to pristine PPy, indicating improved AC conductivity due to enhanced charge carrier hopping at the PPy/WO_3 interfaces [23,42].

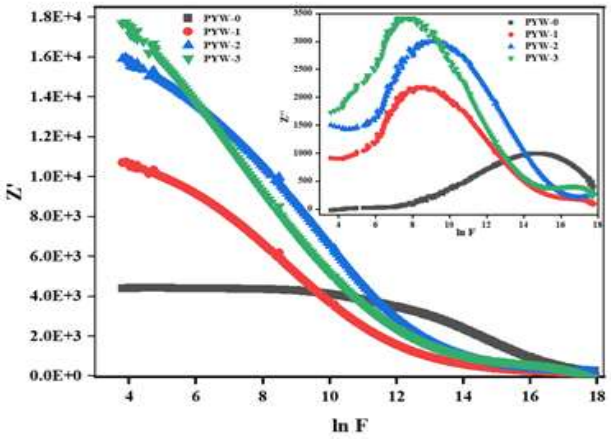

Fig. 9. The real Z′ and imaginary part Z'' (inset) of impedance with frequency for polypyrrole doped with WO3 (X = 0.5, 5, 10, & 15 wt %).

The Z″, ln F plots indicate weak, broad relaxation features in pristine PPy (inset), while the doped nanocomposites exhibit stronger, higher-amplitude Z″ peaks that shift with increasing WO_3 content, suggesting the presence of additional relaxation processes and reduced characteristic relaxation times. The imaginary part of the impedance, Z″, initially increases with frequency, attains a maximum, and subsequently decreases; this peak is indicative of the system's characteristic relaxation time. The PPy-W1 sample (5 wt% WO_3) exhibits a Z″ peak at lower frequencies and with greater amplitude, indicating slower relaxation and more significant resistive effects. In contrast, increased filler loadings enhance conductivity and decrease interfacial resistance, which improves charge mobility and shifts the relaxation peak to higher frequencies [40,41].

The asymmetric characteristics of the Z″ peaks indicate non-Debye relaxation, which is influenced by a range of relaxation times due to structural heterogeneity and grain-boundary effects [23,34]. The impedance response, along with Z′ and electric-modulus analyses, indicates that WO_3 incorporation effectively modifies the electrical and relaxation properties of PPy and improves Maxwell–Wagner–Sillars interfacial polarization and charge-storage capacity, positioning these PPy/WO_3 nanocomposites as viable options for frequency-tunable devices, capacitive sensors, and energy-storage applications [34].

Nyquist plots

The Nyquist plots (Z″ vs. Z′) for PPy/WO_3 nanocomposites (PYW-0 to PYW-3, 0–15 Wt % of WO_3) are shown in fig 10. All of the compositions have depressed semicircular arcs, which show that the bulk and grain boundaries are relaxing. Non-Debye behavior arises from structural heterogeneity and a variation in relaxation times. Undoped PPy (PYW-0) has the smallest semicircle, which means it has the lowest bulk resistance and relatively weak interfacial polarization. The semicircle diameter and the maximum of Z" both go up as the WO_3

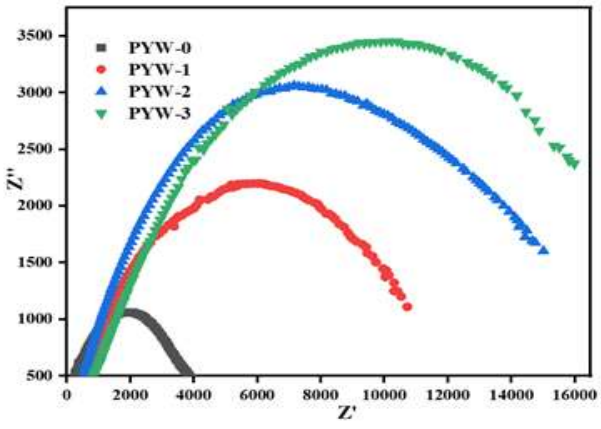

Fig. 10. Nyquist plots for polypyrene doped with WO3 (X = 0.5, 5, 10, & 15 wt %).

content goes up, especially in the 10 and 15 wt% samples. This shows that WO_3 is an insulator, that the Maxwell–Wagner–Sillars interfacial polarization is stronger at the PPy/WO_3 interfaces, and that charge carriers are better able to be trapped. The intermediate composition PYW-1 (5 wt%) exhibits a moderate arc, signifying a balance between sufficient interfacial polarization and relatively continuous conductive pathways; generally, lower Z′ and Z″ values are associated with improved electrical conductivity and expedited relaxation dynamics. In Nyquist representation, each depressed semicircle represents a dominant charge-transfer/interfacial-polarization relaxation process.

The diameter of the semicircle shows the bulk resistance, and its position and shape show the conductivity and dielectric response of the nanocomposite. An equivalent circuit with a series resistance (R_s) and a parallel arrangement of bulk resistance (Rb or Rp) and a constant phase element (CPE) accurately represents the impedance spectra (Fig.11). The CPE acts as an ideal capacitor to account for non-ideal, frequency-dependent capacitive behavior and replicate the depressed arcs. If needed, an extra R–CPE branch can effectively capture explicit interfacial polarization. The Nyquist plots, Z′(f), Z″(f), and electric-modulus analyses show that adding WO_3 changes resistance, interfacial polarization, and relaxation dynamics in a big way. This makes it easier to fine-tune the electrical properties of PPy–WO_3 nanocomposites for use in energy storage, sensors, and high-frequency electronic devices [40,43,44].

IV. CONCLUSION

Polypyrrole/WO_3 nanocomposites were successfully synthesized, as evidenced by XRD analysis, which confirmed the formation of an amorphous PPy matrix embedded with uniformly dispersed nanocrystalline WO_3, exhibiting average crystallite sizes of approximately 61.9–74.5 nm. Dielectric characterization revealed that the incorporation of WO_3 significantly elevates low-frequency permittivity through pronounced Maxwell–Wagner–Sillars interfacial polarization, while both the real (ε′) (highest value for PYW-1 is 14.5) and imaginary (ε″) components of permittivity diminish with increasing frequency.

The AC conductivity, spanning ~10^{-3} to 10^{-1} S·cm^{-1}, increases with frequency in accordance with Jonscher's universal power law, indicating dominant hopping-type charge transport mechanisms. AC conductivity shows increasing trend for pure PPY up to 1MHz frequency and after this frequency WO3 doped PPY shows comparatively higher conductivity then pure PPY and also found decrease in the conductivity for increase in the WO3 concentrations, indicating higher filler concentrations cause nanoparticle agglomeration, increasing interchain distances and hindering the hopping of charge carriers, resulting in lower conductivity.

Impedance and electric modulus analyses further highlighted non-Debye relaxation behavior and a strong dependence of both bulk and interfacial resistances on composite composition. Collectively, these findings demonstrate that precise control of WO_3 loading provides a powerful route to tailor polarization dynamics, relaxation processes, and electrical conduction, positioning PPy/WO_3 nanocomposites as promising candidates for frequency-tunable dielectric components, capacitive sensors, and compact energy storage devices.

REFERENCES

1. Gangopadhyay R, De A. Conducting polymer nanocomposites: A brief overview. Chem Mater 2000;12:608–22. https://doi.org/10.1021/cm990537f.
2. Mane AT, Navale ST, Pawar RC, Lee CS, Patil VB. Microstructural , optical and electrical transport properties of WO 3 nanoparticles coated polypyrrole hybrid nanocomposites. Synth Met 2015;199:187–95. https://doi.org/10.1016/j.synthmet.2014.11.031.
3. Zhu J, Wei S, Zhang L, Mao Y, Ryu J, Karki AB, Young P. Polyaniline-tungsten oxide metacomposites with tunable electronic properties † 2011:342–8. https://doi.org/10.1039/c0jm02090g.

4. Lou J, Zhu X, Yang X, Hao H, Ma D, Zhu L, Wang J. Structure and electrochromic properties of polypyrrole films synthesized by AC electrochemical impedance spectroscopy under different amplitude. Mater Today Commun 2024;39. https://doi.org/10.1016/j.mtcomm.2024.108586.
5. Ananda SR, Kumari L, M.V. M. Temperature-dependent dielectric measurements of polypyrrole/zinc cobalt oxide nanocomposites by impedance spectroscopy. J Alloys Compd 2024;1009. https://doi.org/10.1016/j.jallcom.2024.176894.
6. Tan F, Zhou J, Guo Z, Zhang C, Yu S, Yang Y, Xie Y, Cao X, Wu X, Gao X, Li Z, Qu Y, Li L. Research Progress on Electrochromic Properties of WO 3 Thin Films 2025:1–37.
7. Zheng JY, Sun Q, Cui J, Yu X, Li S, Zhang L, Jiang S, Ma W, Ma R. Review on recent progress in WO3-based electrochromic films: preparation methods and performance enhancement strategies. Nanoscale 2023;15:63–79. https://doi.org/10.1039/D2NR04761F.
8. Ahmad K, Oh TH. Progress in Tungsten Trioxide-Based Materials for Energy Storage and Smart Window Applications. Crystals 2025;15. https://doi.org/10.3390/cryst15010010.
9. Sankar S, Ramesan MT. Synthesis, Characterization, Conductivity and Gas Sensing Performance of Copolymer Nanocomposites Based on Copper Alumina and Poly(aniline-co-pyrrole) 2022. https://doi.org/10.21203/rs.3.rs-1484974/v1.
10. Wang Q, Wu X, Huang J, Chen S, Zhang Y, Dong C, Chen G, Wang L, Guan H. Enhanced microwave absorption of biomass carbon/nickel/polypyrrole (C/Ni/PPy) ternary composites through the synergistic effects. J Alloys Compd 2022;890. https://doi.org/10.1016/j.jallcom.2021.161887.
11. Aryadevi G, Joseph G, Mathew VR, Nair GG, Thomas PC, Joseph A, Joseph GP. Optimizing the electrochemical properties of PPy/ZnO nanocomposites for supercapacitor electrode. J Mater Sci Mater Electron 2024;35. https://doi.org/10.1007/s10854-024-13225-9.
12. El-Nahass MM, Ali HAM, Saadeldin M, Zaghllol M. AC conductivity and dielectric properties of bulk tungsten trioxide (WO 3). Phys B Condens Matter 2012;407:4453–7. https://doi.org/10.1016/j.physb.2012.07.043.
13. Elashmawi IS, Ismail AM, Abdelghany AM. The incorporation of polypyrrole (PPy) in CS/PVA composite films to enhance the structural, optical, and the electrical conductivity. Polym Bull 2023;80:11379–99.
14. Ibrahim B, Saafan SA, Shater REE, Omar MK. Room temperature AC properties and impedance analysis of Mg ferrite/polypyrrole (PPy) and Mg ferrite/reduced graphene oxide (rGO) composites. Indian J Phys 2025;99:1335–45. https://doi.org/10.1007/s12648-024-03372-4.
15. Moolemane R, Rashmi HM, Surekha M, Krishna SBN. In situ synthesis and AC conductivity studies of polypyrrole–cobalt nanocomposites. Acad Mater Sci 2025;2. https://doi.org/10.20935/acadmatsci7554.
16. Rithin Kumar NB, Crasta V, Praveen BM. Dielectric and electric conductivity studies of PVA (Mowiol 10-98) doped with MWCNTs and WO3 nanocomposites films. Mater Res Express 2016;3:1–12. https://doi.org/10.1088/2053-1591/3/5/055012.
17. Al-Sulami AI, Elamin NY, Aldosari E, Farea MO, Alzahrani SS, Al-Harthi AM, Alharbi EM, Rajeh A. Tunable band gap and ionic conductivity in PMMA and PANI blend with WO_3 nanocomposites for optoelectronics and energy storage devices. Sci Rep 2025;15:34543. https://doi.org/10.1038/s41598-025-17880-8.
18. Erdönmez S, Karabul Y, Kılıç M, Güven Özdemir Z, Esmer K. Structural characterization and dielectric parameters of polyindole/WO3 nanocomposites. Polym Compos 2021;42:1347–55. https://doi.org/10.1002/pc.25905.
19. Riaz M, Mehmood A, Ali SM, Wahab R, Alotaibi R, Ali SD. Synthesis of metal sulfide-based ZrS2/rGO–PPy nanocomposites for high-temperature memory devices: Structural, morphological, thermal, and dielectric insights. Micro and Nanostructures 2026;209:208439. https://doi.org/10.1016/j.micrna.2025.208439.
20. Mu W, Xie X, Li X, Zhang R, Yu Q, Lv K, Wei H, Jian Y. Wo3. Mater Lett 2015;138:107–9.

https://doi.org/https://doi.org/10.1016/j.matlet.2014.09.113.
21. Zhu J, Wei S, Zhang L, Mao Y, Ryu J, Mavinakuli P, Karki AB, Young DP, Guo Z. Conductive polypyrrole/tungsten oxide metacomposites with negative permittivity. J Phys Chem C 2010;114:16335–42. https://doi.org/10.1021/jp1062463.
22. El-Khiyami SS, Hafez RS. Dielectric study and Cole–Cole plots of poly(methyl methacrylate) doped with nanostructured metal oxides. J Polym Res 2021;28:396. https://doi.org/10.1007/s10965-021-02754-0.
23. Bharathi M, Anuradha KN, Murugendrappa M V. Structural, AC conductivity, dielectric and impedance studies of polypyrrole/praseodymium calcium manganite nanocomposites. Dig J Nanomater Biostructures 2023;18:343–65. https://doi.org/10.15251/DJNB.2023.181.343.
24. Hiremath A, Pattar J, Chandra SS, Rao HNA, Sreekanth R, Mahendra K, Manohara SR. Facile Design of PANI/G-CN/WO3 Nanocomposites with Integrated Photocatalytic and Dielectric Functionalities. J Phys Chem Solids 2025:113305. https://doi.org/https://doi.org/10.1016/j.jpcs.2025.113305.
25. Wang L, Yang J, Cheng W, Zou J, Zhao D. Progress on Polymer Composites With Low Dielectric Constant and Low Dielectric Loss for High-Frequency Signal Transmission. Front Mater 2021;Volume 8-.
26. Sood Y, Singh K, Mudila H, Lokhande PE, Singh L, Kumar D, Kumar A, Mubarak NM, Dehghani MH. Insights into properties, synthesis and emerging applications of polypyrrole-based composites, and future prospective: A review. Heliyon 2024;10:e33643. https://doi.org/https://doi.org/10.1016/j.heliyon.2024.e33643.
27. Ashwajeet JS, Sankarappa T. Dielectric and AC conductivity studies in Li2O-CoO-B2O3-TeO2 glasses. Ionics (Kiel) 2017;23:627–36. https://doi.org/10.1007/s11581-016-1819-6.
28. Anju C, Palatty S. Electrochimica Acta Ternary doped polyaniline-metal nanocomposite as high performance supercapacitive material 2019;299:626–35. https://doi.org/10.1016/j.electacta.2019.01.030.
29. Vijeth H, Yesappa L, Niranjana M, Ashokkumar SP, Devendrappa H. Investigation on structural, optical and electrical properties of polythiophene-Al2O3 composites. AIP Conf. Proc., vol. 1953, American Institute of Physics Inc.; 2018. https://doi.org/10.1063/1.5032663.
30. Jayakrishnan P, Ramesan MT. Studies on the effect of magnetite nanoparticles on magnetic , mechanical , thermal , temperature dependent electrical resistivity and DC conductivity modeling of poly (vinyl alcohol- co -acrylic acid)/ Fe 3 O 4 nanocomposites. Mater Chem Phys 2016:1–10. https://doi.org/10.1016/j.matchemphys.2016.11.028.
31. Mane AT, Navale ST, Mane RS, Naushad M, Patil VB. Progress in Organic Coatings Synthesis and structural , morphological , compositional , optical and electrical properties of DBSA-doped PPy – WO 3 nanocomposites. Prog Org Coatings 2015;87:88–94. https://doi.org/10.1016/j.porgcoat.2015.05.007.
32. Migahed MD, Ishra M, Fahmy T, Barakat A. Electric modulus and AC conductivity studies in conducting PPy composite films at low temperature. J Phys Chem Solids 2004;65:1121–5. https://doi.org/https://doi.org/10.1016/j.jpcs.2003.11.039.
33. Ahmed K, Kanwal F, Ramay SM, Atiq S, Rehman R, Ali SM, Alzayed NS. Composites with Exceptional Dielectric Behaviour 2018. https://doi.org/10.3390/polym10111273.
34. Anuradha KN, Murugendrappa M V. Structural , DC Conductivity and Electric Modulus Studies of Polypyrrole Praseodymium Manganite Nanocomposites 2023;61:165–74. https://doi.org/10.56042/ijpap.v61i3.70065.
35. Kudryashov MA, Logunov AA, Mochalov LA, Kudryashova YP, Trubyanov MM, Barykin A V., Vorotyntsev I V. Hopping conductivity and dielectric relaxations in ag/pan nanocomposites. Polymers (Basel) 2021;13. https://doi.org/10.3390/polym13193251.
36. Tsangaris GM, Psarras GC, Kouloumbi N. Electric modulus and interfacial polarization in

composite polymeric systems. J Mater Sci 1998;33:2027–37. https://doi.org/10.1023/A:1004398514901. .

37. Li X, He S, Jiang Y, Wang J, Yu Y, Liu X, Zhu F, Xie Y, Li Y, Ma C, Shen Z, Li B, Shen Y, Zhang X, Zhang S, Nan C-W. Unraveling bilayer interfacial features and their effects in polar polymer nanocomposites. Nat Commun 2023;14:5707. https://doi.org/10.1038/s41467-023-41479-0.
38. Atta A, Alotiby MF, Al-Harbi N, El-Aassar MR, Uosif MAM, Rabia M. Fabrication, Structural Properties, and Electrical Characterization of Polymer Nanocomposite Materials for Dielectric Applications. Polymers (Basel) 2023;15. https://doi.org/10.3390/polym15143067.
39. Analysis I. Dielectric properties, Impedance Analysis, and Electrical Conductivity of Ag Doped Radiation Grafted Polypropylene 2017;30:95–107.
40. Mane AT, Navale ST, Patil VB. Room temperature NO2 gas sensing properties of DBSA doped PPy–WO3 hybrid nanocomposite sensor. Org Electron 2015;19:15–25. https://doi.org/https://doi.org/10.1016/j.orgel.2015.01.018.
41. Abbas Y, Abbas A. Dielectric and gas sensing properties of in situ electrochemically polymerized PPy-MgO-WO3 nanocomposite films. Iraqi J Sci 2021;62:2915–34. https://doi.org/10.24996/ijs.2021.62.9.8.
42. View of Raman spectroscopy and electrical properties of polypyrrole doped dodecylbenzene sulfonic acid_Y2O3 composites.pdf n.d.
43. Electrical, Dielectric Property and Electrochemical Performances of Plasticized Silver Ion-Conducting Chitosan-Based Polymer NanocompositesM. Hadi J, B. Aziz S, M. Nofal M, Hussein SA, Hafiz MH, Brza MA, Abdulwahid RT, Kadir MFZ, Woo HJ. Electrical, Dielectric Property and Electrochemical Performances of Plasticized Silver Ion-Conducting Chitosan-Based Polymer Nanocomposites. Membranes (Basel) 2020;10. https://doi.org/10.3390/membranes10070151.
44. Khalil HF, Elsharkawy SG, Al-harby NF. Dielectric and Magnetic Properties for Microwave Applications 2024:1–14.